A R C H I V E S O F M E T A L L U R G Y A N D M A T E R I A L S
Volume 60 2015 Issue 2
DOI: 10.1515/amm-2015-0184

J. KONSTANTY*, A. ROMAŃSKI*,♯, E. BACZEK**, D. TYRALA*

NEW WEAR RESISTANT IRON-BASE MATRIX MATERIALS FOR THE FABRICATION OF SINTERED DIAMOND TOOLS

NOWE, ODPORNE NA ZUŻYCIE ŚCIERNE MATERIAŁY NA BAZIE ŻELAZA PRZEZNACZONE DO PRODUKCJI SPIEKÓW NARZĘDZIOWYCH METALICZNO-DIAMENTOWYCH

The possibility of the use of inexpensive iron-base powders in the production of sintered diamond tools is again explored. Ball-milled Fe-Ni-Cu-Sn-C and Fe-Mn-Cu-Sn-C powders were consolidated to a virtually pore-free condition by hot pressing at 900°C. The resultant materials are characterised by a combination of high Knoop hardness, 260-440 and yield strength, 780-1350 MPa, and resistance to abrasion. These properties can be significantly modified by changing the milling time.
Keywords: ball milling, sintered diamond tools, matrix powder, Fe-Ni-Cu-Sn-C, Fe-Mn-Cu-Sn-C, hot pressing

W artykule zamieszczono wyniki badań nad możliwością zastosowania tanich proszków na bazie żelaza do produkcji spiekanych narzędzi metaliczno-diamentowych. Mielone proszki Fe-Ni-Cu-Sn-C i Fe-Mn-Cu-Sn-C poddano prasowaniu na gorąco w temperaturze 900°C. Otrzymane spieki posiadają gęstość zbliżoną do teoretycznej, wysoką twardość (260-400 HK0.5), granicę plastyczności (780-1350 MPa) oraz dużą odporność na zużycie ścierne. Wymienione własności są w dużym stopniu uzależnione od czasu mielenia proszków wyjściowych.

1. Introduction

The prices of synthetic diamond grits continue to decline as production technology becomes more cost effective. This provides a strong incentive for producers of sintered diamond tools to reduce the cost of metallic powders for the matrix wherein the diamonds are embedded. The main focus of attention is on tools dedicated to process abrasive materials, where the matrix properties are customised by adding expensive WC, or WC/W_2C, to accommodate specific wear conditions [1].

Until relatively recently it has been a common practice to use fine Co-WC powders, with up to 60% WC, for the fabrication of diamond-impregnated tool components used to cut/grind abrasive sandstone, fresh concrete, asphalt, porous ceramics, etc. Although cobalt and its substitutes [2-4] are still used for special tools, the latest trend is towards a broader application of premixed and ball milled iron-base powders [5]. Seemingly, the most suitable candidates are ferrous alloys with nickel or manganese, copper, tin and carbon.

2. Experimental methods and results

Basing on earlier studies [6-8], Fe-Ni-Cu-Sn-C and Fe-Mn-Cu-Sn-C alloys from inexpensive raw powders were chosen as potential Co-WC substitutes for the manufacture of sintered diamond impregnated tools for abrasive applications. Spongy iron, carbonyl nickel, milled ferro-manganese, water atomised tin-bronze and synthetic graphite powders, provided by Höganäs AB, Vale, ESAB, ECKA and Timcal, respectively, were the starting powders (Fig. 1, Table 1).

TABLE 1
Chemical compositions and mean particle sizes of the starting powders

Powder grade	Chemical composition [wt.%]						Mean particle size [μm]
	Fe	Mn	Ni	Cu	Sn	C	
NC100.24	100	-	-	-	-	-	85 (1)
T210	-	-	bal	-	-	0.33	0.6 (2)
XH1210	bal	80	-	-	-	7.0	134 (1)
XH1218	bal	80.5	-	-	-	1.5	143 (1)
25GR80/20-325		-	-	bal	20.6	-	23 (1)
F10	-	-	-	-	-	100	<10 (2)

(1) sieve analysis
(2) Fisher sub-sieve size

The powders were premixed in appropriate proportions (Table 2), in a chaotic motion mixer, for 10 minutes and subsequently ball milled in air, at 65% critical speed, for 8 and 120 hours. About 50% of the milling container was filled with 12 mm 100Cr6 steel balls and 10:1 ball-to-powder weight ratio was used.

* AGH-UNIVERSITY OF SCIENCE & TECHNOLOGY, AL. A. MICKIEWICZ 30, 30-059 KRAKÓW, POLAND
** INSTITUTE OF ADVANCED MANUFACTURING TECHNOLOGY, 37A WROCLAWSKA STR., 30-011 KRAKÓW, POLAND
♯ Corresponding author: aromanski@agh.edu.pl

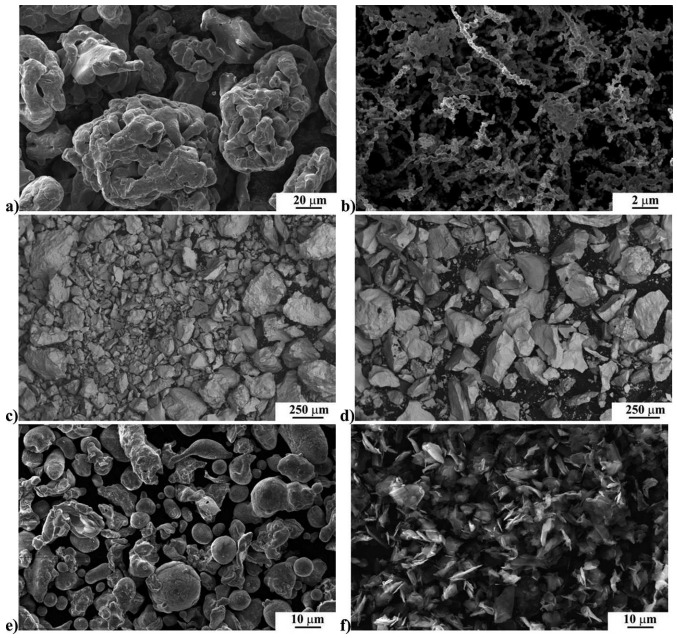

Fig. 1. Experimental powders: NC100.24 iron (a), T210 nickel (b), XH1210 ferromanganese (c), XH1218 ferromanganese (d), 25GR80/20-325 bronze (e) and TIMREX F10 graphite (f)

TABLE 2
Chemical compositions of ball milled powders

Powder designation	Starting mix composition [wt.%]	Chemical composition [wt.%]					
		Fe	Mn	Ni	Cu	Sn	C
Fe-Ni	T210 - 12% 25GR80/20-325 - 8% F10 - 0.63% NC100.24 - bal	bal	-	12	6.4	1.6	0.67
Fe-Mn	25GR80/20-325 - 8% XH1210 - 7.5% XH1218 - 7.5% NC100.24 - bal	bal	12	-	6.4	1.6	0.64

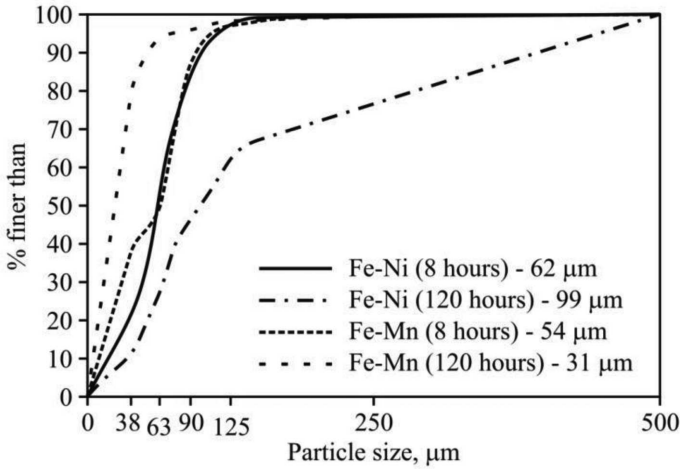

Fig. 2. Particle size distributions of the ball milled powders plotted cumulatively. The mean particle sizes (weighted arithmetic means) are listed in the legend

After milling, the powders were subjected to sieve analysis (Fig. 2) and examined microscopically by scanning electron (SEM) and light (LM) microscopy (Fig. 3).

The ball milled powders were then poured into four rectangular cavities of a graphite mould and consolidated to a virtually pore-free condition by passing an electric current through the mould under an uniaxial compressive load. The powders were held at 900°C for 3 minutes, under 25 MPa (Fe-Ni-Cu-Sn-C) or 35 MPa (Fe-Mn-Cu-Sn-C), and subsequently cooled to room temperature.

All as-sintered specimens were first tested for density using the Archimedes' principle. Two specimens of each material were used for Knoop hardness tests, microstructural observations and X-ray diffraction (XRD) phase analysis using Cu Kα radiation. Knoop hardness numbers and the proportion of (γFe) to (αFe) in the subsurface layer were evaluated during preparation of the metallographic specimens on surfaces ground on SiC #220 paper and again after final polishing with 1 μm diamond (Table 3).

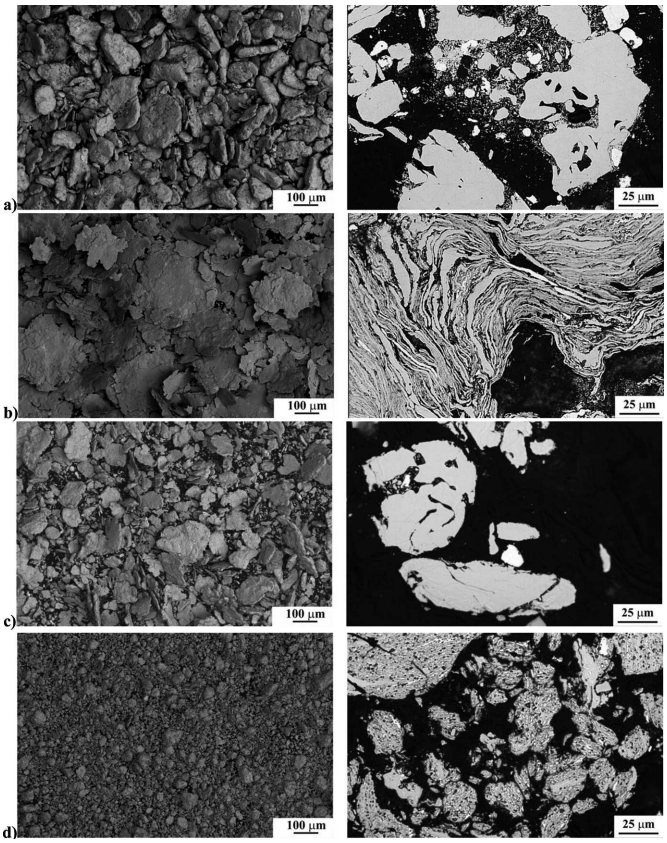

Fig. 3. Particle shape (left) and microstructure (right) of Fe-Ni (a, b) and Fe-Mn powders (c, d) after milling for 8 (a, c) and 120 hours (b, d)

The remaining two specimens of each alloy were cut in two, to produce four bars which were subjected to 3-point bending in order to determine the 0.2% offset yield strength (OYS), the transverse rupture strength (TRS) and the amount of plastic deformation at failure (ε_{pl}).

TABLE 3

Densities, Knoop hardness numbers and volume percentages of austenite [3]

Material	Milling time [hours]	Density [g/cm^3]	KH0.5		$V_{(\gamma Fe)}$ [vol.%] [4]	
			as-polished condition	as-ground condition	as-polished condition	as-ground condition
Fe-Ni-8	8	7.90±0.09	258±36	305±50	83	12
Fe-Ni-120	120	7.62±0.10	440±18	442±54	27	10
Fe-Mn-8	8	7.75±0.01	298±17	359±35	73	63
Fe-Mn-120	120	7.61±0.08	363±31	391±52	96	98

[3] scatter intervals estimated at 90% confidence level

[4] estimated assuming that $V_{(\alpha Fe)} + V_{(\gamma Fe)} = 100\%$ (no account taken of other phases)

TABLE 4

Bend properties and abrasion resistance indices of the experimental alloys [5]

Material	Milling time [hours]	Oxygen [wt.%]	Carbon [wt.%]	3-point bending test			Ai [μm/20m]
				TRS [MPa]	OYS [MPa]	ε_{pl} [%]	
Fe-Ni-8	8	0.29±0.02	0.57±0.01	1161±277	775±178	2.0±1.0	22.0±3.1
Fe-Ni-120	120	1.77±0.08	0.59±0.01	584±247	-	0.1±0.1	39.1±6.5
Fe-Mn-8	8	0.68±0.03	0.67±0.01	1325±228	866±41	2.2±1.4	23.2±4.3
Fe-Mn-120	120	1.30±0.08	0.64±0.01	1421±65	1351±155	0.8±1.3	28.4±5.4
Co-20%WC	-	-	-	-	-	-	33.6±8.2

[5] scatter intervals estimated at 90% confidence level

The fracture surfaces were subsequently examined by SEM (Fig. 4) and the broken test bars were used to evaluate the oxygen and carbon content using the LECO combustion analysers, and to produce abrasive wear test pieces. The wear measurements were performed under 3-body abrasion conditions on the Micro Wear Test (MWT) instrument [9]. The abrasive index (Ai), representing the average loss of height of the test piece per 20 m sliding distance, was calculated for abrasion by standardized quartz sand. In addition to the Fe-Ni and Fe-Mn materials, a commercial Co-20%WC PM alloy was tested as reference (Table 4).

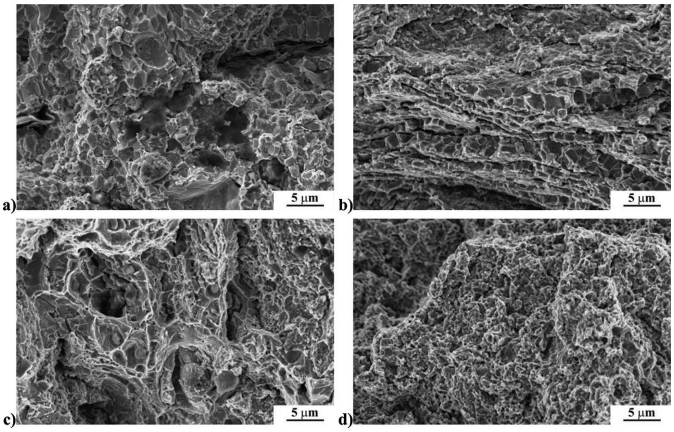

Fig. 4. SEM fractographs of the Fe-Ni-8 (a), Fe-Ni-120 (b), Fe-Mn-8 (c) and Fe-Mn-120 alloy (d)

The microstructures of the experimental alloys were examined and analysed by means of a SEM fitted with an energy dispersive spectroscopy (EDS) system (Figs 5-7).

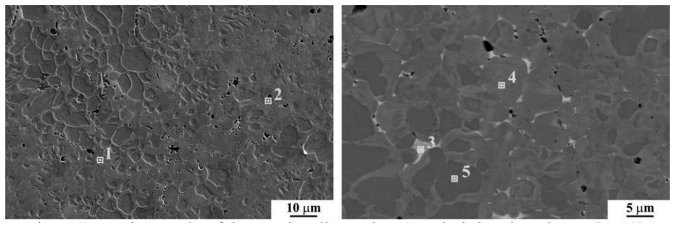

Fig. 5. SEM micrographs of the Fe-Ni-8 alloy and EDS analysis in selected areas [wt.%]: 1 and 3: Fe_2O_3; 2: 52Cu-35Sn-8Ni-5Fe; 4: 82Fe-14Ni-4Cu; 5: Fe

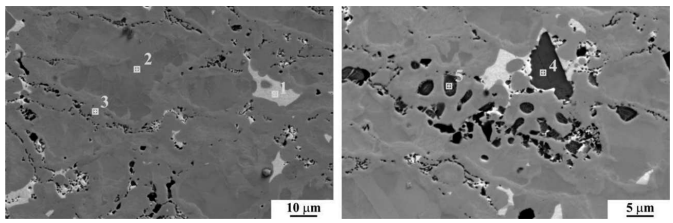

Fig. 6. SEM micrographs of the Fe-Mn-8 alloy and EDS analysis in selected areas [wt.%]: 1: 64Cu-20Sn-12Mn-5Fe; 2: Fe; 3: 79Fe-19Mn-2Cu; 4 and 5: Mn_2O_3

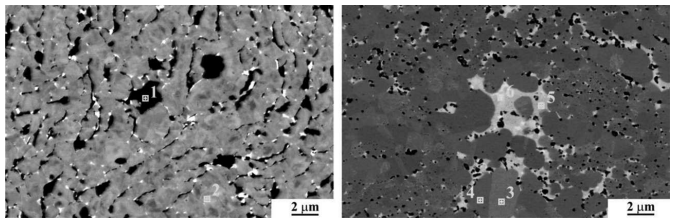

Fig. 7. SEM back scattered electron (BSE) images of the Fe-Ni-120 (a) and Fe-Mn-120 alloy (b)

In addition to the microstructure and properties of the matrix, it was equally important to check to what extent synthetic diamond interacted with the tested materials when exposed to elevated temperature during the hot pressing cycle. To this end, high-grade diamond grits were electrochemically extracted from segments consolidated for 3 minutes at 900°C and examined using a stereomicroscope (Fig. 8) and SEM (Fig. 9).

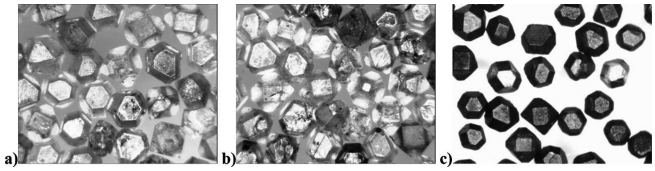

Fig. 8. Diamond grits in as-delivered condition (a) and extracted from the Fe-Ni-8 (b) and Fe-Mn-8 matrix (c)

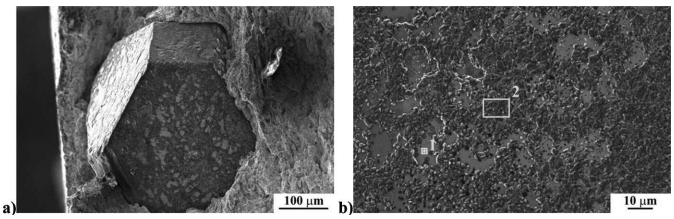

Fig. 9. Diamond crystal embedded in the Fe-Mn-8 matrix (a) and EDS analysis of its surface (b) [wt.%]: 1: 100C; 2: 95.4C-4.6Fe

3. Discussion and conclusions

The results in Table 3 indicate that the tested ball-milled powders can be hot pressed to near-full density by a 3-minute hold at 900°C under a pressure of 25-35 MPa. Apparently the addition of bronze to the powders prior to milling provides a sufficient amount of liquid at 900°C to aid densification. During milling, the powder particles are repeatedly welded together, fractured, re-welded, etc. After 120 hours of milling the Fe-Ni-Cu-Sn-C powder shows a flaky shape and a characteristic layered microstructure with very fine lamellar spacing (Fig. 3b). In contrast, the Fe-Mn-Cu-Sn-C powder particles flatten during the early stages of milling (Fig. 3c), but, due to heavy working, particle fracturing soon prevails over welding, resulting in finer (Fig. 2) and more equiaxed particles after milling for 120 hours (Fig. 3d).

After consolidation, the alloys possess high hardness, which markedly increases with milling time. Except for Fe-Ni-120, the other three materials show an excellent combination of high strength and ductility (Table 4), and a pronounced strain hardening response to abrasion as indicated by the Knoop hardness results (Table 3). From the XRD data (Table 3), it is evident that the Fe-Ni-8 alloy strain hardens due to the abrasion-induced martensitic reaction (γFe)→ (αFe), whereas in the Fe-Mn-8 and Fe-Mn-120 alloys only a small portion of austenite, if any, can be transformed to martensite under tribological straining. This implies that other mechanisms, such as mechanical twinning [10], may contribute to strain hardening during abrasion. Interestingly, the wear performance (on this testing method) of Fe-Ni-8 and Fe-Mn-8 is markedly better than that of the commercial Co-20%WC reference material, which is extensively used to manufacture tools which process abrasive stones and ceramics.

The metallographic observations (Figs 5-7) reveal marked differences in grain size and microstructural inhomogeneity of the various specimens. Generally, the microstructure refines with milling time, but retains chemical microinhomogeneity, as observed on the BSE SEM images (Fig. 7). Since the ball-milling operation is performed in air, the powders pick up from around 0.3 to almost 1.8% oxygen after milling for 8 and 120 hours, respectively. Apparently the Fe-Ni powders are more prone to oxidation during milling due to the relatively high content (12 wt.%) of very fine carbonyl nickel powder having large specific surface area. This results in a very high content of fairly course oxides in the Fe-Ni-120 alloy (Fig. 7a). The Fe-Ni powder particle flatness and degree of oxidation increase progressively with milling time. This leads to an undesirable oriented lamellar structure of the Fe-Ni-120 material, which seems to promote its brittle breakage along the oxide networks (Fig. 4c).

It still remains unclear why prolonged milling decreases the volume density of retained austenite in Fe-Ni-120 (Table 3), whereas similar milling conditions render the Fe-Mn powder virtually austenitic upon consolidation. This presumably results in a strengthened material with better retention of ductility and resistance to abrasion, as compared to Fe-Ni-120 (Table 4).

The visual inspection of diamonds extracted from the Fe-Ni-8 matrix shows no evidence of graphitisation and harmful reactions occurring at the diamond-matrix interface (Figs 8a and 8b). Conversely, the Fe-Mn-8 matrix promotes surface graphitisation (Fig. 8c) and formation of metallurgical bonds between the matrix and diamond crystals without adversely affecting the crystal shape and edge sharpness (Fig. 9).

In conclusion, it can be stated that:

1. Ball-milling proves to be an economical means of producing Fe-Ni-Cu-Sn-C and Fe-Mn-Cu-Sn-C powders which have layered microstructures with a very fine lamellar spacing.
2. These powders are readily consolidated to virtually pore-free condition by a 3-minute hold at 900°C under a moderate pressure of 25-35 MPa.
3. The amount of austenite in these alloys and its stability strongly depend on powder composition and milling time.
   - In nickel-containing alloys, the largest amounts of retained austenite have been detected in material produced from the powder ball-milled for 8 hours. Milling prolonged to 120 hours led to excessive oxidation of the powder and a threefold decrease in the austenite content of the as-consolidated material. The retained austenite is unstable and can be partly transformed to high-carbon martensite under tribological straining.
   - In manganese-containing alloys, the amounts of retained austenite increase in proportion to other phases with powder milling time. The greatest volume fraction is reached in the material produced from the powder ball-milled for 120 hours. The retained austenite seems to be stable and resists severe cold working by abrasion.

4. The Fe-Ni-8 and Fe-Mn-8 alloys appear to show superior resistance to abrasion over their commercial wear resistant Co-20%WC equivalent.
5. The strain-induced martensitic reaction taking place in the Fe-Ni-8 alloy increases its wear resistance and, by generating compressive stress under the working face of the tool, may (hypothetically) improve retention of working diamonds.
6. The Fe-Ni-8 matrix is neutral to diamond, whereas Fe-Mn-8 mildly promotes surface graphitisation and formation of metallurgical bonds which are desirable for better diamond retention [11,12].

Acknowledgements

The authors gratefully acknowledge Professor W. Ratuszek and Mrs H Ciaś for their able assistance with the XRD and LECO, respectively. The work was supported by the Dean of the Faculty of Metals Engineering & Industrial Computer Science AGH through contract No 11.11.110.299.

Received: 20 September 2014.

REFERENCES

[1] J. Konstanty, Powder Metallurgy **49**, 299 (2006).
[2] Anon., Marmo Macchine International **18**, 156 (1997).
[3] I.E. Clark, B-J. Kamphuis, Industrial Diamond Review **62**, 177 (2002).
[4] B-J. Kamphuis, A. Serneels, Industrial Diamond Review **64**, 26 (2004).
[5] J. Konstanty, Powder Metallurgy **56**, 184 (2013).
[6] D. Tyrala, Doctoral Thesis. AGH-University of Science & Technology, Krakow 2010.
[7] J. Konstanty, T.F. Stephenson, D. Tyrala, Diamond Tooling Journal **3**, 26 (2011).
[8] A. Romanski, J. Konstanty, Archives of Metallurgy and Materials **59**, 189 (2014).
[9] J.S. Konstanty, D. Tyrala, Wear **303**, 533 (2013).
[10] S. Allain et al., Materials Science and Engineering A **387-389**, 158 (2004).
[11] A. Romanski, J. Lachowski, J. Konstanty, Industrial Diamond Review **66**, 43 (2006).
[12] A. Romanski, Archives of Metallurgy and Materials **55**, 1073 (2010).